View metadata, citation and similar papers at core.ac.uk

brought to you by CORE

provided by Elsevier - Publisher Connector

PERGAMON

Available online at www.sciencedirect.com

SCIENCE DIRECT®

Vision Research 43 (2003) 2333–2344

Vision Research

www.elsevier.com/locate/visres

Alterations of L- and M-cone driven ERGs in cone and cone–rod dystrophies

Hendrik P.N. Scholl [a,b], Jan Kremers [a,*,1]

[a] *Department of Pathophysiology of Vision and Neuroophthalmology, University Eye Hospital, 72076 Tübingen, Germany*
[b] *Institute of Ophthalmology, Moorfields Eye Hospital, London, EC1V 2PD, UK*

Received 10 November 2002

Abstract

To study the L- and M-cone pathways and their interactions in patients with cone and cone–rod dystrophies, ERG responses were measured to stimuli which modulated exclusively the L- or the M-cones, or the two simultaneously. The L- and M-cone driven ERG amplitudes were considerably reduced in the patients. The mean phases of the L-cone driven ERGs in the patients lagged those of normals significantly, whereas the mean M-cone driven ERGs were significantly phase advanced resulting in a substantial phase difference between the two ERG responses. These phase changes in the L- and M-cone driven responses in the patients cannot be detected with standard ERG techniques.
© 2003 Elsevier Ltd. All rights reserved.

Keywords: Cone dystrophy; Cone–rod dystrophy; Electroretinography; L-cones; M-cones

1. Introduction

Progressive cone and cone–rod dystrophies are a subgroup of the inherited retinal dystrophies. The diagnosis is established by electrophysiological evaluation. Patients with cone and cone–rod dystrophies typically exhibit visual acuity loss, visual field impairment, color vision disturbances, photophobia, a reduction of the photopic ERG amplitude that is proportionally larger than for the scotopic ERGs, and sometimes nystagmus (Berson, Gouras, & Gunkel, 1968; Birch & Fish, 1987; Fishman, 1976; Goodman, Ripps, & Siegel, 1963; Krill, 1977; Krill, Deutman, & Fishman, 1973; Ripps, Noble, Greenstein, Siegel, & Carr, 1987; Szlyk, Fishman, Alexander, Peachey, & Derlacki, 1993; Yagasaki & Jacobson, 1989). The clinical, psychophysical and electroretinographical parameters can show substantial variability. Moreover, genetic studies have revealed numerous genetic subtypes with different modes of genetic transmission. Genes responsible for autosomal dominant (*CRX*, *GUCA1A*, *GUCY2D*, *HRG4*, *PDE6B*, *peripherin/RDS*), autosomal recessive (*ABCA4*, *RDH5*, *RHO*), and X-linked (*RPGR*) cone and cone–rod dystrophies have been mapped and cloned. Due to this heterogeneity, various methods for classifying cone and cone–rod dystrophies have been proposed (for a review see, Simunovic & Moore, 1998): cone and cone–rod dystrophies have been classified on the basis of the mode of inheritance, psychophysical testing or electroretinography. However, a single mutation can be associated with multiple phenotypes, e.g. in the *peripherin/RDS* gene (Weleber, Carr, Murphey, Sheffield, & Stone, 1993). On the other hand, patients with the same apparent phenotype, characterized by standard methods, do not necessarily share the same gene defect. To investigate the cone and cone–rod dystrophies in more detail we therefore need better methodologies.

To study whether different cone types and their postreceptoral mechanisms are selectively affected, ERG measurements using differently colored stimuli have been conducted (e.g. Kellner & Foerster, 1992, 1993). By means of such color-stimulated ERGs, a predominant S-cone dystrophy (Bresnick, Smith, & Pokorny, 1989; van Schooneveld, Went, & Oosterhuis, 1991) and a predominant L-cone dystrophy (Kellner, Sadowski, Zrenner, & Foerster, 1995; Reichel, Bruce, Sandberg, & Berson,

* Corresponding author. Address: Department of Experimental Ophthalmology, University Eye Hospital, Röntgenweg 11, 72076 Tübingen, Germany. Tel.: +49-7071-2985031; fax: +49-7071-295777.
E-mail address: jan.kremers@uni-tuebingen.de (J. Kremers).
[1] Present address: Novartis Ophthalmics, 4002 Basel, Switzerland.

0042-6989/$ - see front matter © 2003 Elsevier Ltd. All rights reserved.
doi:10.1016/S0042-6989(03)00411-5

1989) have been described. But, in none of the mentioned studies a complete separation of responses driven by the different cone types was achieved. This is especially true for the differentiation between the L- and M-cone driven pathways, because the absorption spectra of the L- and M-cones overlap considerably (Stockman, MacLeod, & Johnson, 1993). A separation of signals driven by different cone types is possible in combination with chromatic adaptation. Chromatic adaptation procedures have been used in ERG recordings (Padmos & van Norren, 1971; van Norren & Padmos, 1973). But, although the ERG responses driven by the adapted or desensitized cone type in such procedures may often be very small, they may not be negligible. More importantly, comparison between measurements at different states of adaptation are nearly impossible, because adaptation is an inherent non-linearity that will push the retina into a different mode of operation.

We therefore developed a method with which ERG responses to cone isolating stimuli and to stimuli in which the L- and M-cones are stimulated simultaneously with known contrasts are measured without changing the overall state of adaptation (Kremers, Usui, Scholl, & Sharpe, 1999; Usui, Kremers, Sharpe, & Zrenner, 1998a, 1998b). Our technique is reminiscent of the silent substitution paradigm (for a review see, Estévez & Spekreijse, 1982) and of the heterochromatic flicker photometry ERG (Jacobs, Neitz, & Krogh, 1996; Neitz & Jacobs, 1984). The method has been used to investigate the L- and M-cone driven ERGs in patients with rod–cone dystrophy or retinitis pigmentosa (RP; the two terms may be used synonymously, see, Krill, 1977; Scholl & Kremers, 2000), Stargardt macular dystrophy (Scholl, Kremers, Vonthein, White, & Weber, 2001) and Best macular dystrophy (Scholl, Kremers, Apfelstedt-Sylla, & Zrenner, 2000). Here we provide data on the L- and M-cone driven ERGs in a prospective cross-sectional study of patients that have been diagnosed by standard techniques to have cone and cone–rod dystrophies.

2. Methods

2.1. Patients with cone and cone–rod dystrophies and normal subjects

Thirteen patients (age 10–43 years, median = 15 years) were included in the study. A detailed history (including family history), ophthalmologic examination (including slit lamp biomicroscopy, funduscopic evaluation by retinal biomicroscopy and fundus photography, visual acuity), visual fields (Tübingen Automated Perimeter), color vision tests (Lanthony D-15 saturated/desaturated test), and Ganzfeld electroretinography according to the ISCEV standard (Marmor & Zrenner, 1998) were recorded and formed the basis for the diagnosis of cone and cone–rod dystrophy. Patients were included when they exhibited responses in the photopic standard 30-Hz flicker ERG that were considerably above the noise level. Such a criterion introduces a bias because patients with severe cone and cone–rod dystrophies were possibly excluded; we have been able to show that extreme phase differences between L- and M-cone driven ERGs can result in substantially reduced standard 30-Hz white flicker ERGs (Scholl & Kremers, 2000; Scholl et al., 2001) and such patients might have been also excluded because their standard flicker ERG was near the noise level. In accordance with Krill (Krill, 1977), our inclusion criteria for cone and cone–rod dystrophy were defined by a reduced photopic standard Ganzfeld ERG with either a normal (cone dystrophy) or reduced (cone–rod dystrophy) scotopic standard Ganzfeld ERG (rod-specific b-wave to the 24 dB attenuated standard flash) in combination with the absence of signs of any acquired retinal disorder. The amplitude reduction of the photopic b-wave was proportionally larger than that of the rod-specific b-wave. Typically, there were additional signs of cone disturbance that were in accordance with cone and cone–rod dystrophy such as visual field impairment, color vision disturbances or visual acuity loss (Krill, 1977).

Color vision was screened by the Lanthony D-15 desaturated test (Lanthony & Dubois, 1973). This arrangement test allows an evaluation of color vision disorders. A discrimination between protan and deutan color vision deficiencies is virtually not possible, whereas a discrimination between tritan and protan/deutan deficiencies is easily achieved. We described the results of this arrangement test by a categorization scheme from normal (no error, I), insignificant (one or more adjacent tablets confused, II), significant (two confusions between non-adjacent tablets, III), very significant (numerous confusions along one major axis: Protan/Deutan or Tritan, IV), chaotic (V), and arrangements not feasible (i.e. because the patient was not able to discriminate any differences in color, VI) (Nimsgern, Krastel, Auffarth, Eggers, & Lang, 1998).

Twenty-nine normal subjects (age 9–57 years, median = 27 years) served as a control. More detailed ERG data on a subpopulation of the normal subjects have been published previously (Kremers et al., 1999). Informed consent was obtained from all subjects, and the study was conducted with the approval of our institutional ethical committee in human experimentation.

2.2. ERG recording

The method of ERG recording has been described before (Kremers et al., 1999; Usui et al., 1998a). Briefly, the stimuli were presented on a computer controlled monitor (BARCO CCID 121) driven at 100 Hz by a

VSG 2/3 graphics card (Cambridge Research System). The monitor subtended 124° by 108° at the 10 cm viewing distance. We used 30 Hz square wave modulation of the red, green, and blue phosphor with predefined Michelson contrasts. The modulation of cone excitation was quantified by the cone contrast ($100\% \times ((E_{max} - E_{min})/(E_{max} + E_{min}))$, where E_{max} and E_{min} are the maximal and minimal cone excitations respectively). The time averaged luminance of the monitor was 66 cd/m^2 (40 cd/m^2 for the green phosphor, 20 cd/m^2 for the red phosphor, and 6 cd/m^2 for the blue phosphor). The excitation in each cone type by the monitor phosphors was calculated by multiplying the phosphor emission spectra with the psychophysically based fundamentals (Stockman et al., 1993). The time averaged chromaticity in CIE (1964) large field coordinates, the total retinal illuminance, and the photoreceptor illuminance for the L-cones, M-cones, S-cones, and rods have been published elsewhere (Kremers, Stepien, Scholl, & Saito, 2003) and are freely available under http://journalofvision.org/3/2/3/, Table 1. The modulation of cone excitation was quantified by the Michelson cone contrast and defined the stimulus strength for each cone type separately. The S-cones were silently substituted in all conditions (S-cone contrast was 0%). In 19 of the 29 normal subjects, we measured ERG responses to 32 different stimuli: eight conditions of different L-/M-cone contrast ratios (1:1; −1:1; 1:2; 0:1; 2:1; −2:1; −1:2: 1:0) with four contrasts at each condition (100%, 75%, 50% and 25% of the maximally possible cone contrast). An L- to M-cone contrast ratio of 1:1 corresponds to an in-phase modulation of the L- and M-cones with equal cone contrast; an L- to M-cone contrast ratio of −1:1 corresponds to a modulation of the two cone types in counter-phase with equal cone contrast; an L- to M-cone contrast ratio of 1:2 corresponds to an in-phase modulation of the two cone types with the M-cone contrast twice as the L-cone contrast; and an L- to M-cone contrast ratio of 0:1 corresponds to a silent substitution of the L-cones. In 13 patients and in 10 of the 29 normal subjects, we limited the measurements to four conditions with L-/M-cone contrast ratios of 1:1, 1:0, 0:1, and −1:1 which allowed us to obtain relatively reliable amplitude data and simultaneously direct measurements of response phases under cone isolating stimuli. The term 'L- and M-cone driven ERGs' is used to refer to the responses originating in the L- and the M-cones including the subsequent post-receptoral stages.

ERG recordings were obtained from one eye for all subjects. Since cone and cone–rod dystrophies usually affect both eyes homogeneously, one eye was randomly chosen (in both subject groups). The pupils of the controls were dilated with 0.5% tropicamide, those of the patients with both 0.5% tropicamide and 5% phenylephrine. The pupil diameter was measured before each experiment; there was no significant difference in pupil diameter between the two subject groups. The eyes were kept light-adapted at average room illumination for at least 10 min before ERG recording.

Corneal ERG responses were measured with DTL fiber electrodes which were positioned on the conjunctiva directly beneath the cornea and attached with their two ends at the lateral and nasal canthus. The reference and ground electrodes (gold cup electrodes) were attached to the ipsilateral temple and the forehead, respectively. The signals were amplified and filtered between 1 and 300 Hz (Grass Instruments Co.) and sampled at 1000 Hz with a National Instruments AT-MIO-16DE-10 data acquisition card. ERG responses to 12 runs, each lasting four seconds, were averaged in each measurement.

Table 1
Characteristics of the 13 patients with cone and cone–rod dystrophies: patient number, gender, age at examination [years], age of onset [years; from birth = B], visual symptoms (reduction of visual acuity = 1; photophobia = 2; color vision disturbances = 3; night blindness = 4), evidence of progression by history (H) or by repeated examinations (E), nystagmus, visual acuity, score from the Lanthony D-15 desaturated test (CV; T indicates errors along the tritanopic confusion line; P/D indicates errors in the protan/deutan directions), modes of genetic transmission (autosomal dominant = AD; autosomal recessive = AR; simplex = S), and diagnosis (based on the standard ERG; see Table 2)

Nr	Sex	Age	Onset	Symptoms	Prog	Nystagmus	VA	CV	Heredity	Diagnosis
1	m	43	12	1, 2, 3	H, E	No	0.05	IV (P/D)	AR	Cone–rod dystrophy
2	f	16	8	1, 3	H, E	No	0.05	VI	S	Cone–rod dystrophy
3	m	10	2	1, 3	H, E	Yes	0.1	V	AR	Cone dystrophy
4	f	38	6	1, 2, 4	H, E	No	0.1	VI	S	Cone–rod dystrophy
5[a]	m	15	6	1	H, E	No	0.6	IV (T)	AD	Cone dystrophy
6	m	37	32	1, 2	H	No	0.05	VI	AR	Cone dystrophy
7	f	12	6	1	H, E	No	0.5	II	S	Cone–rod dystrophy
8	f	14	6	1	H, E	No	0.3	II	S	Cone–rod dystrophy
9	f	30	3	1, 2, 3, 4	E	Yes	0.1	V	S	Cone–rod dystrophy
10	m	26	B	1, 2, 3	H	No	0.2	VI	AD	Cone dystrophy
11	f	14	6	1, 2, 3, 4	H	No	1/35	V	AR	Cone dystrophy
12	m	13	7	1, 2	H	No	0.1	V	AR	Cone–rod dystrophy
13	m	12	B	1, 2, 3	E	No	0.3	IV (P/D)	AR	Cone dystrophy

[a] Patient #5 carried the Gly170Ser mutation in the *peripherin/RDS* gene.

2.3. Statistical analysis

Data were analyzed by JMP© 4.0.2 computer program (SAS Institute, Inc., Cary, NC, USA 2000). Results with p-values less than 0.05 were considered statistically significant.

3. Results

3.1. Group characteristics and standard ERGs

The patients were significantly younger than the controls ($p = 0.04$, Wilcoxon rank-sum test). Subject groups did not differ in their fraction of male to female subjects ($p = 1.0$, two-tailed Fisher's exact test). The clinical data of the patients are shown in Table 1.

By definition, the patients with cone and cone–rod dystrophies exhibited reduced photopic b-waves. In the majority of the patients, the implicit times of the photopic b-wave (8 out of 13 patients) and of the 30-Hz flicker ERG (12 out of 13 patients) were prolonged. Six patients exhibited rod-specific ERG b-waves (to the 24 dB attenuated standard flash) within normal limits (and by definition were diagnosed as cone dystrophy), whereas the amplitude was reduced in the remaining 7 patients (and thus were diagnosed to have cone–rod dystrophy). For the maximal combined response to the standard flash, 9 patients showed reduced amplitudes of the a-wave and 10 showed prolonged implicit times; the amplitude of the b-wave was reduced in 10 patients and the implicit time prolonged in 6 patients. The results of the standard ERGs are presented in Table 2.

3.2. L- and M-cone driven ERG responses and model fits

Fig. 1 shows the ERG responses to four stimulus conditions: (1) to in-phase modulation of the L- and the M-cones (L:M cone contrast ratio 1:1; 76.8% contrast in each cone type; the positive contrast ratio indicates that two cone types are excited in phase), (2) to pure L-cone modulation (L:M cone contrast ratio 1:0; 24.7% L-cone contrast), (3) to pure M-cone modulation (L:M cone contrast ratio 0:1; −31.2% M-cone contrast), and (4) to counter-phase modulation of the two cone types (L:M cone contrast ratio −1:1; the negative contrast ratio indicates that two cone types are excited in counter-phase, 13.8% M-cone contrast and −13.8% L-cone contrast) for a normal subject (left column) and two patients (middle and right column). For each stimulus condition, ERG responses to four contrasts (100%, 75%, 50% and 25% of the maximally possible cone contrast) were measured. In Fig. 1, the ERG responses to the maximal cone contrast at each condition are displayed.

Patient #5 carried the Gly170Ser mutation in the *peripherin/RDS* gene; the patient's genotype was previously reported (Kohl et al., 1998). The patient shows a cone dystrophy with reduced amplitudes of the standard cone driven ERGs in combination with normal implicit times (Table 2). Patient #4 with a cone–rod dystrophy exhibited reduced amplitudes of the standard cone driven ERGs in combination with a delayed 30-Hz flicker

Table 2
The results of the scotopic and photopic ERGs (amplitude [μV] and implicit times [ms]) according to the ISCEV standard: rod-specific b-wave to the 24 dB attenuated standard flash, a- and b-wave of the maximal combined response to the standard flash, cone-specific b-wave, and 30-Hz white flicker ERG

Nr	Rod-specific ERG		Maximal combined response				Cone specific ERGs			
	Rod b-wave		a-wave		b-wave		Cone b-wave		30-Hz flicker ERG	
	Amplitude	Imp. time	Amplitude	Imp. time	Amplitude	Imp. time	Amplitude	Imp. time	Amplitude	Imp. time
1	**107**	**100.0**	206	17.0	**326**	37.6	**37**	**33.2**	**29**	**33.6**
2	**68**	**104.0**	**109**	**20.5**	**325**	44.0	**23**	**36.6**	**28**	**36.9**
3	223	**123.0**	338	**26.0**	738	**50.5**	**56**	29.4	**32**	**34.2**
4	**81**	**96.0**	**96**	**23.0**	**168**	**51.5**	**48**	30.8	**22**	**35.1**
5	148	**112.0**	**90**	**22.5**	**226**	**49.0**	**39**	27.3	**17**	30.3
6	188	71.0	**142**	**19.5**	**252**	43.0	**38**	**36.6**	**10**	**35.1**
7	**26**	**108.0**	**43**	**24.0**	**147**	47.5	**13**	31.0	**17**	**41.8**
8	**111**	82.5	**83**	18.0	**194**	**55.0**	**83**	**34.2**	**18**	**33.3**
9	**60**	89.5	**70**	17.5	**189**	46.5	**19**	31.8	**31**	**32.7**
10	149	**96.0**	189	**19.0**	**282**	41.0	**25**	**40.2**	**12**	**35.1**
11	188	**99.5**	**134**	**22.5**	377	**59.0**	**47**	**35.8**	**30**	**36.9**
12	**133**	82.5	**141**	**22.0**	**239**	**56.0**	**21**	**33.6**	**17**	**33.5**
13	189	85.0	165	**19.0**	351	42.0	**11**	**33.4**	**18**	**33.4**
Norm 5th	140	78	163	15.5	343	36	97	27.7	47	27.2
Norm 95th	339	94.5	347	17.5	638	48.3	223	32.8	112	32.2

The two rows in the bottom provide normative values (5th‰ and 95th‰ of the amplitudes and implicit times). Abnormal findings are bold.

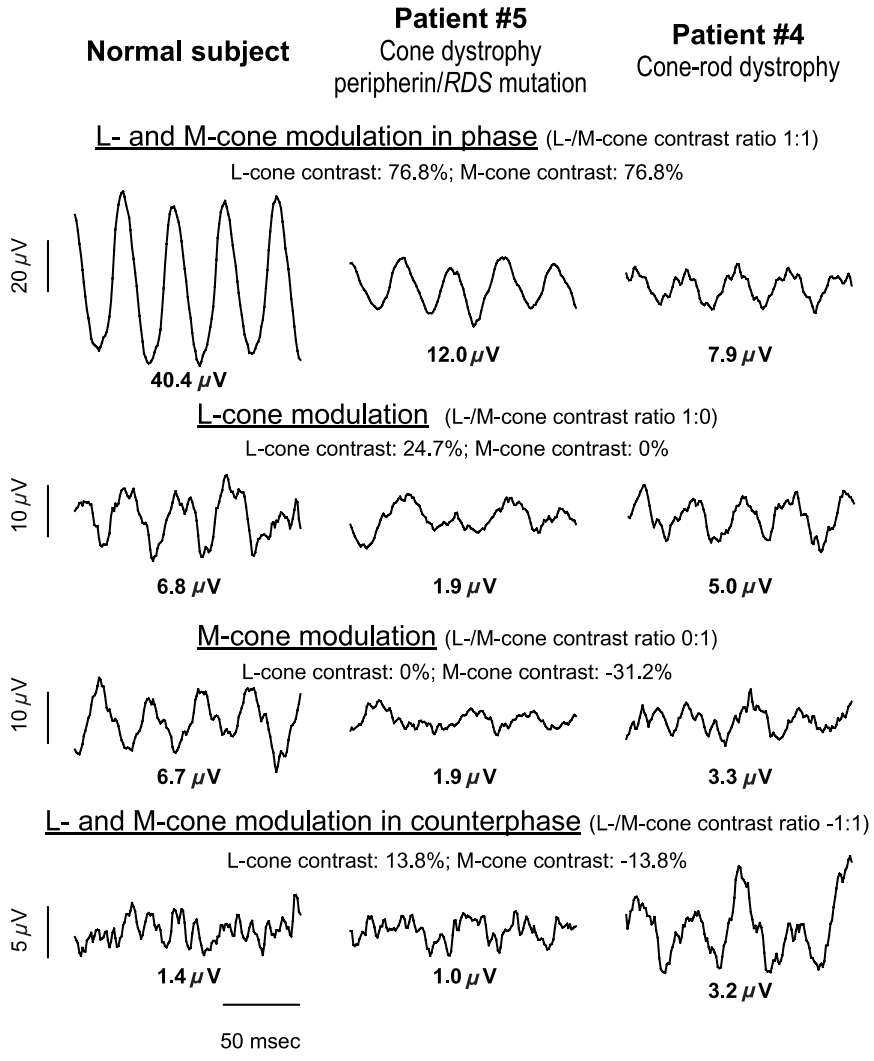

Fig. 1. Averaged ERG responses to in-phase modulation of the L- and the M-cones (upper row; L:M cone contrast ratio 1:1; 76.8% L-cone contrast; 76.8% M-cone contrast), to pure L-cone modulation (second row; L:M cone contrast ratio 1:0; 24.7% L-cone contrast; 0% M-cone contrast), to pure M-cone modulation (third row; L:M cone contrast ratio 0:1; 0% L-cone contrast; −31.2% M-cone contrast), and to counter-phase modulation of the two cone types (lower row; L:M cone contrast ratio 1:−1; 13.8% L-cone contrast; −13.8% M-cone contrast) for a normal subject (left column) and two patients with cone and cone–rod dystrophy, respectively (#5 and #4; second and third column; patient #5 carried a Gly170Ser mutation of the *peripherin/RDS* gene. The ERG signals are 150 ms extracts out of 4 s traces, that are the averages of 12 runs. The traces are from the same time windows of the recordings, enabling a mutual comparison. Positive and negative cone contrasts indicate in-phase and counter-phase modulation with the red monitor phosphor respectively, which was used to synchronize the stimulus with the data acquisition. Drift components in the ERG responses to the L- and M-cone isolating stimuli were suppressed by removing low frequency components. Next to each trace, the ERG response amplitude [μV] is given that was obtained by Fourier analysis.

response (Table 2). Several aspects of these original ERG tracings are of interest. In the normal observer, the responses to in-phase modulation of the L- and the M-cones (amplitude, 40.4 μV; obtained from Fourier analysis, see below) are much larger than to counter-phase modulation (1.4 μV) and to the L-cone (6.8 μV) and M-cone isolating stimuli (6.7 μV). The amplitude difference cannot be fully attributed to the larger cone contrasts in the in-phase condition (the different scaling of the ordinate partially compensates for the different cone contrasts; as is stated below, there is a linear relationship between cone contrast and ERG amplitude), suggesting that the responses originating in the L- and M-cones interact additively. Thus for counter-phase modulation (lower panel), the signals originating in the L- and the M-cones almost cancel out each other. Apart from an overall lower response amplitude, the same is true for patient #5 (second column; 12.0 and 1.0 μV for in-phase and counter-phase modulation, respectively). Patient #4 (third column), however, exhibited larger ERG signals for the counter-phase modulation (when compensating for differences in cone contrast; 3.2 μV for 13.8% L-cone contrast/−13.8% M-cone contrast) than for the in-phase modulation (7.9 μV for 76.8% L-cone contrast/76.8% M-cone contrast) indicating *subtractive* interactions between the L- and M-cone driven ERG signals.

The ERG responses were Fourier analyzed and the ERG response amplitudes and phases were defined as the amplitudes and phases of the fundamental component. We found an approximately linear relationship between ERG response amplitude and cone contrast at all conditions for the patients with cone and cone–rod dystrophies and for the normal subjects (Kremers & Scholl, 2001; Kremers et al., 1999; Usui et al., 1998a). The slope of the linear regression to the amplitude data is the increase in ERG amplitude per percent increase in cone contrast. This slope was used to define the cone contrast gain and quantifies the ERG sensitivity. The inverse of the cone contrast gain is the cone contrast increase needed for a 1 μV response increase, which, owing to the linear relationship between amplitude and cone contrast, is equivalent to a threshold. The cone contrast gains and the thresholds were obtained for all ratios of L- to M-cone contrasts. Fig. 2A shows the measured ERG thresholds for two normal subjects (N7 and N22). The ellipses are fits of a model, based on the assumption that the ERG responses are the results of a vector summation of the ERG signals originating in the L- and M-cones. A detailed description of the model can be found elsewhere (Kremers et al., 1999). Briefly, we assume that the signals originating in the L- and the M-cones have separate weightings (defined by the cone contrast gains) and phases, and that the total response is simply the addition of the two separate responses at each instant. Because the responses are basically sinusoidal without intrusion of higher harmonics (see also, Usui et al., 1998b), they can be expressed as vectors, the lengths of which are determined by the amplitudes; the angles with the positive x-axis are equivalent to the phases. As a result of the above mentioned assumption, the response vector to a combination of L- and M-cone modulation equals the addition of the two response vectors obtained with the cone isolating conditions. In the fits of this model to the threshold data, there are three free parameters: the L-cone weighting or L-cone contrast gain (A_L), the M-cone weighting or the M-cone contrast gain (A_M), and the absolute phase difference between the L- and the M-cone driven ERG responses ($|P_L - P_M|$). Thus, the model fits to the threshold data allow the estimation of the ratios of L-/M-cone weighting. Furthermore, the absolute phase difference between the L- and M-cone driven ERGs can be compared with the difference in response phases measured directly with the cone isolating stimuli.

3.3. L- and M-cone driven ERG weightings and ERG sensitivity in patients

Fig. 2B shows the ERG thresholds for six patients (In a subset of 7 patients, it was not possible to obtain an ERG threshold for every stimulus condition because the responses were unreliably small, resulting in three or less thresholds: This number of thresholds we considered to be too low for a reliable model fit, and therefore disre-

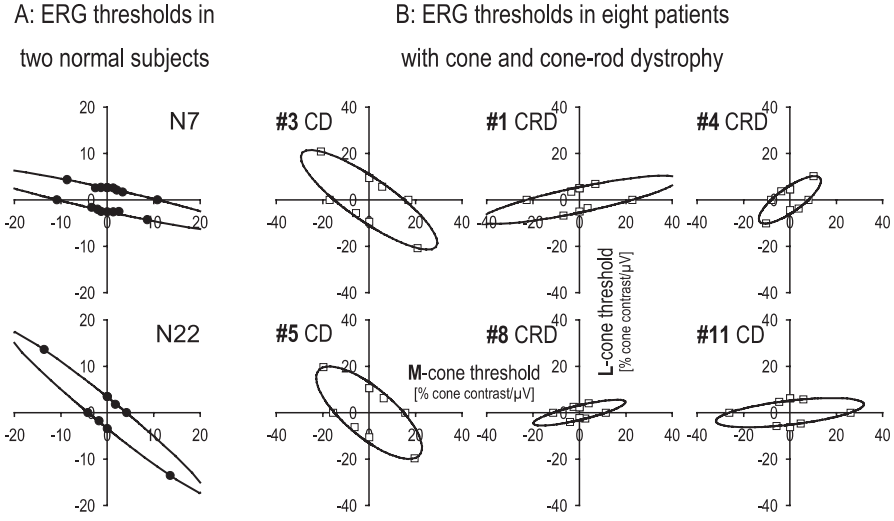

Fig. 2. Threshold contrasts in two normal subjects (N7 and N22; A) and six patients with cone and cone–rod dystrophies (B). The ellipses are fits of a vector addition model to the data points (Kremers et al., 1999). A threshold contrast increase for a 1 μV ERG response increase was determined at each condition (for calculation see formula (2) in Kremers et al. (1999)). The abscissa defines L-cone threshold (the inverse of the contrast gain), and the ordinate defines M-cone threshold [%cone contrast/μV]. The phase difference between L- and M-cone driven ERG responses varies considerably between individual patients. As in the normal subjects, a subset of the patients (#3, #5) displayed ellipses with the major axis oriented within the second and fourth quadrant indicating phase differences below 90° resulting in a *additive* interaction between the signals originating in the L-cones and the M-cones (patient #5 carried a Gly170Ser mutation of the *peripherin/RDS* gene). The ellipses of another subset of the patients (#1, #4, #8, #11), however, were oriented within the first and third quadrant indicating phase differences above 90° resulting in a *subtractive* interactions. In all of these six patients, most ERG thresholds were considerably larger than in the normal subjects corresponding to a decreased ERG sensitivity (note the different scaling between normals and patients). (Please note the different scaling.)

garded the model fits in those cases. In this subset of 7 patients the data analysis was restricted to the original ERG recordings, i.e. the ERG amplitudes and phases). The L- and M-cone weightings (A_L and A_M, respectively) estimated from the model fits to the threshold data were statistically analyzed with an analysis of variance (ANOVA). The average A_L (0.293) and A_M (0.112) of the normal subjects were significantly larger than the average A_L (0.11) and A_M (0.06) of the patients ($p < 0.0001$ and $p = 0.01$, respectively; $n = 6$). Within the subject groups, the difference between A_L and A_M was significant for both the normal subjects ($p < 0.0001$) and the patients ($p = 0.017$). A subsequent Bonferroni-Holm-test (to correct for multiple comparisons; multiple $\alpha = 0.05$) revealed that all these differences were significant.

From the cone weightings, we calculated the individual L-/M-cone weighting ratios. As has been reported previously for normal subjects (Kremers et al., 1999), and patients with RP (Scholl & Kremers, 2000), Stargardt macular dystrophy (Scholl et al., 2001), and Best macular dystrophy (Scholl et al., 2000), there is a considerable inter-individual variability of the L-/M-cone weighting ratio reflected by the different orientations of the ellipses. The larger the L-/M-cone weighting ratio the more the thresholds ellipses are tilted towards the M-cone axis. This variability can be correlated with variations in the L-/M-cone weighting ratios in psychophysical tasks tapping the luminance channel and probably can be attributed to the variability in the number of L- and M-cones in the human retina (Kremers et al., 2000; Williams & Roorda, 1999). The L-/M-cone weighting ratios are not normally distributed, making a standard test difficult. We therefore converted the ratios into their logarithms to give the data a normal distribution. An unpaired t-test on these data did not reveal a significant difference ($p = 0.46$; $t = 0.7$; $n = 6$) between the ratios in the patients and the controls suggesting a balanced decrease of the L- and M-cone driven ERGs in cone and cone–rod dystrophies.

Because of the large inter-individual variability of L- and M-cone weightings, neither of them can be directly used to quantify the overall L-/M-cone driven ERG sensitivity of individual patients. We therefore quantified the mean maximal sensitivity, S_m, by determining the theoretically least threshold defined as the smallest possible distance of the fitted ellipse to the origin. This smallest possible distance can be estimated analytically from the model fits (or derived from the thresholds for individual conditions in case that the model fit was not feasible) (Scholl & Kremers, 2000; Scholl et al., 2000). The mean maximal L-/M-cone driven ERG sensitivity thus takes into account possible phase differences between the two ERG pathways which is not the case for the standard ERG (Scholl & Kremers, 2000; Scholl et al., 2001). S_m in the patients' group ($n = 13$) was significantly lower than in the control group ($p < 0.0001$; $t = 8.1$; Fig. 3). The two subgroups (cone dystrophy and cone–rod dystrophy patients) did not differ in S_m ($p = 0.1528$; $t = -1.6$).

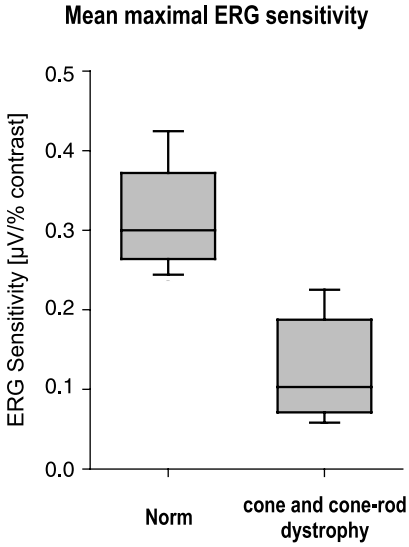

Fig. 3. Mean maximal L-/M-cone driven ERG sensitivity (quantified by the smallest possible distance of the fitted ellipse to the origin) for the normal subjects and the patients. The means are given by the horizontal marks within the boxes, the boxes indicate the 25th‰ and 75th‰, error bars the 5th‰ and 95th‰. The mean maximal sensitivity of the patients with cone and cone–rod dystrophies was significantly reduced.

3.4. L- and M-cone driven ERG phases

The major axes of the ellipses of all normal subjects are located within the second and fourth quadrant, indicating additive interactions between the signal originating in the L- and M-cones and that the absolute phase difference $|P_L - P_M|$ is always smaller than 90° (Fig. 2). Two out of six patients (#3 and #5 in Fig. 2B) showed ellipse orientation that were similar to those of the normal subjects suggesting *additive* interactions between the L- and M-cone driven ERGs. For patient #5, the model fit confirms the preliminary conclusions drawn from the traces shown in Fig. 1. The two patients displayed normal rod-specific ERG responses and therefore were diagnosed to have a cone dystrophy. However, the distance of the fitted ellipse to the origin was considerably larger reflecting a reduced ERG sensitivity (S_m). In contrast, another subset of four out of six patients (#1, #4, #8, with cone–rod dystrophy and #11 with cone dystrophy in Fig. 2B) exhibited ellipses with major axis located within the first and third quadrant indicative for *subtractive* interactions between the ERG signals arising in the L- and M-cones. For patient #4, these data confirm the preliminary conclusions drawn from the original ERG traces (Fig. 1).

From the Fourier analysis on the ERG responses to the cone isolating stimuli we were able to obtain a direct estimate of the L- and M-cone driven ERG response phases. As discussed previously (Usui et al., 1998b), the actual phases can differ by integer multiples of 360° from the phases obtained from the Fourier analysis. We therefore assumed that the response phases of the patients were as close as possible to those of the normal subjects (Scholl & Kremers, 2000). For the ensuing statistical analysis this was the worst case scenario. We cannot exclude that the responses in the patients are advanced or delayed by integer multiples of 360° which however, seems very unlikely, because that would introduce additional phase delays and advances corresponding to implicit time shifts of at least 33 ms. In Fig. 4, the ERG response phases are shown as a function of cone contrast separately for the M- and L-cone isolating stimuli for all 13 patients. The phase data were only included when the response amplitudes were significantly above noise level (typically being 0.3 μV). As has been observed previously (Usui et al., 1998b; Wu, Burns, & Elsner, 1995), the ERG response phase increased (and thus the phase lag decreases) linearly with increasing cone contrast for the normal subjects within the range of used cone contrasts. This was also true for the L-cone driven ERGs in all patients for whom at least three data points were obtained. However, the M-cone driven ERG phases of only one patient (#8) exhibited a distinctly positive correlation with cone contrast, whereas three patients (#1, #5, #13) showed a distinctly negative correlation.

We applied an analysis of covariance (ANCOVA) to these phase data to correct for the influence of cone contrast. We assumed that the variability in the data can be explained by four factors: subject group (normal subjects; patients, $n = 13$), cone type, cone contrast, and subject number as a random effect (representative for individual differences). Further, it was assumed that these factors could interact, that all measurement errors are identical, and that there is a linear relationship between response phase and cone contrast. As a result, four different straight lines were estimated describing the relationship between response phase and cone contrast for each subject group and each cone type by the ANCOVA (similarly to a procedure described by Scholl et al., 2001). Model fit was good (adj. $R^2 = 0.74$; root mean square error = 19.9°). The influence of cone contrast on the ERG phase data was highly significant ($p < 0.0001$). Subject groups differed significantly ($p = 0.016$) and there was a significant inter-individual variability ($p < 0.0001$). There were interactions between cone type and subject group ($p < 0.0001$) and between cone type and cone contrast ($p = 0.0001$). The combined interaction between subject group, cone type and cone contrast was also significant ($p = 0.003$). The L-cone driven ERG response phase increased significantly with

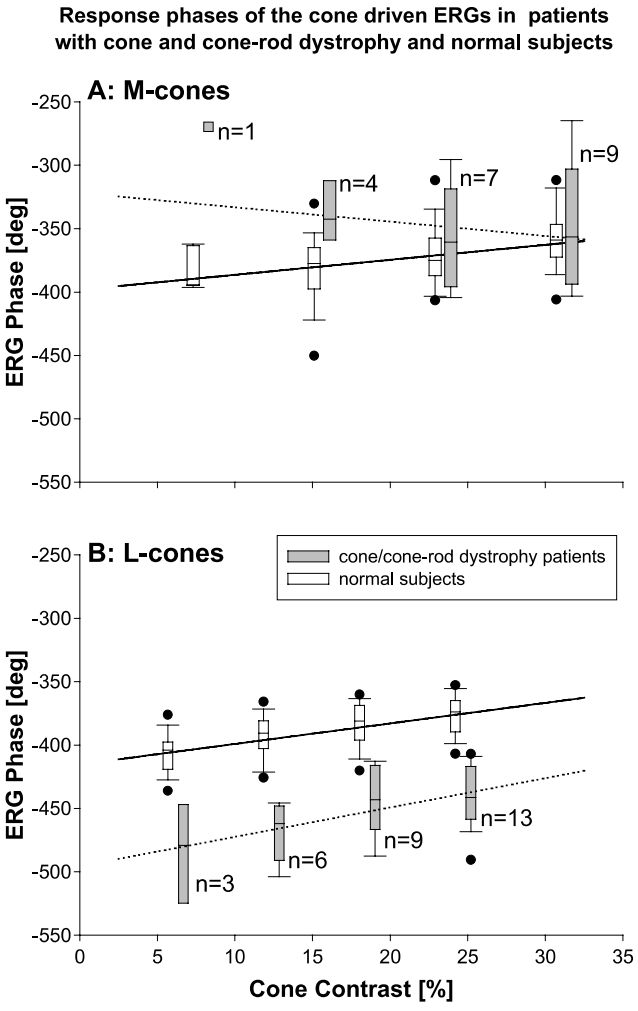

Fig. 4. ERG response phase to cone isolating stimuli as a function of cone contrast in normal subjects and patients with cone and cone–rod dystrophies. Boxes indicate the 25th‰ and 75th‰, error bars the 5th‰ and 95th‰, and points the 1st‰ and 99th‰. The lines describe the relationship between response phase and cone contrast for each subject group and each cone type estimated from the ANCOVA. A: Phase data for M-cone isolating stimuli. The relationship between phase and cone contrast can be described as follows: normal subjects: $f(c) = 1.18$ [deg/%] $* c$ [%] $- 398$ [deg] (solid line); patients: $f(c) = -0.82$ [deg/%] $* c$ [%] $- 329$ [deg] (dotted line). B: Phase data for L-cone isolating stimuli. Observe that the Y-axis has the same range as for the M-cone data. The relationship between phase and cone contrast can be described as follows: normal subjects: $f(c) = 1.62$ [deg/%] $* c$ [%] $- 415$ [deg] (solid line); patients: $f(c) = 2.17$ [deg/%] $* c$ [%] $- 489$ [deg] (dotted line). For clarity, the patient data are shifted 0.5% to larger cone contrast and the data on the normals are shifted 0.5% to smaller cone contrasts.

increasing cone contrast with a slope of 1.62 (SE = 0.27; $p < 0.0001$) in the normal subjects and a slope of 2.17 (SE = 0.62; $p = 0.0003$) in the patients. The M-cone driven ERG response phases also increased with increasing cone contrast in the normal subjects with a slope of 1.18 (SE = 0.34; $p = 0.0006$) but decreased in the patients with a slope of −0.81 (SE = 0.67); this decrease, however, was not significant ($p = 0.09$).

From the ANCOVA, the mean ERG response phase, P_L and P_M (at 19% global mean cone contrast) was estimated for each combination of subject group and cone type as described previously (Scholl et al., 2001). Post-hoc-tests (Tukey-Kramer HSD; $\alpha = 0.05$) revealed that P_L of the patients (−451°; SE = 6°) lagged P_L of the controls (−385°; SE = 4°) significantly and that P_M of the patients (−343°; SE = 8°) was significantly phase advanced compared to the control group (−376°; SE = 4°). P_L and P_M differed significantly in the patients but not in the normal subjects. The similarity between P_L and P_M in the normal subjects can be observed from comparison of the data displayed in Fig. 4A and B. As a cause of the differential effect of cone and cone–rod dystrophy on P_L and P_M, the mean phase difference of 108° (corresponding to 10.0 ms when assuming that a difference in time delay is causing the phase difference) was considerably larger than the one in the normal subjects (9°; corresponding to 0.8 ms delay difference). But again, inter-individual differences were observed, so that in some patients the phase difference was less than 90° and in others larger than 90°. This is in qualitative agreement with the above mentioned finding that the fitted ellipses to the threshold data have a major axis in the second and fourth quadrant (additive interactions; phase difference less than 90°) in some patients and a major axis in the first and third quadrant (subtractive interactions; phase difference larger than 90°) in others. To pursue this issue, we independently estimated the absolute phase differences between L- and M-cone driven ERGs ($|P_L - P_M|$) from the model fits to the threshold data. $|P_L - P_M|$ differed significantly between patients and controls ($p < 0.0001$; unpaired t-test). The absolute phase differences obtained directly from the cone isolating stimuli and those estimated from the model fits were positively correlated ($r = 0.89$; 95% confidence interval 0.78–0.94; mean difference = 1°; SD of the difference = 23°).

We observed a trend between $|P_L - P_M|$ and the amplitude of the rod b-wave: the lower the scotopic ERG amplitude, the larger was the phase difference between the L- and M-cone driven ERGs. We performed a subgroup analysis on the phase difference (obtained from the model fits) for patients with normal rod-specific b-waves (cone dystrophy), reduced rod-specific b-waves (cone–rod dystrophy) and for patients with rod–cone dystrophy. The data of the rod–cone dystrophy patients were obtained from previous measurements in which the same method was employed (Scholl & Kremers, 2000). As shown in Fig. 5, the phase difference between L- and M-cone driven ERGs obtained from patients with cone dystrophy did not overlap with those obtained from patients with cone–rod dystrophy. It is also obvious that there is a trend towards larger phase differences with increasing rod involvement which means that the mean phase difference was smallest for patients with cone dystrophy (66°) and largest for patients with rod–cone dystrophy (161°). An ANOVA showed that the three groups differ significantly ($p = 0.002$; $F = 3.7$).

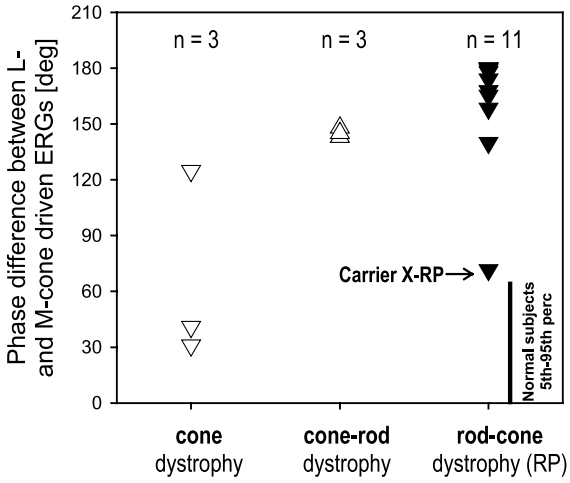

Fig. 5. Subgroup analysis for the phase difference between L- and M-cone driven ERGs for the three groups: cone dystrophy, cone–rod dystrophy, and rod–cone dystrophy (RP). The data of the RP patients have been recently reported (Scholl & Kremers, 2000). An ANOVA showed that the three groups differ significantly ($p = 0.002$; $F = 3.7$). The bar in the lower right corner indicates the normative values (5th ‰, 0.1°; 95th‰, 63.6°) obtained in 29 normal subjects (Kremers et al., 1999). In the RP patients, one female carrier of X-RP exhibited a phase difference that was smaller than those of the other RP patients, but still outside the normal range (Scholl & Kremers, 2000).

4. Discussion

In a recent study on the L- and M-cone driven ERG responses we have shown the complex origin of the standard 30-Hz flicker ERG (Scholl et al., 2001). In a statistical analysis, the amplitude of the 30-Hz flicker ERG according to the ISCEV standard was positively correlated with S_m but negatively correlated with $|P_L - P_M|$ whereas the implicit time of the standard 30-Hz flicker ERG was positively correlated with $|P_L - P_M|$ but negatively correlated with S_m in a large population of Stargardt macular dystrophy patients. In the present patient population with cone and cone–rod dystrophies, all patients exhibited both delayed L-cone driven ERG phases and increased standard 30-Hz flicker ERG implicit times (with the exception of patient #5, see above). This correspondence can be explained on the basis of two observations: first, all patients were L-cone dominated (L-/M-cone ratio range, 1.1–5.1) and second, the mean phase lag of the L-cone driven ERG (66°) was larger than the mean phase advance of the M-cone driven ERG (33°).

Our study shows that an increase in implicit time of the standard 30-Hz flicker ERG in cone and cone–rod

dystrophies must not be interpreted as an indicator for uniformly altered temporal characteristics in all cone type specific pathways. As can be seen in Fig. 4, only the L-cone driven ERG responses were delayed in most patients with cone and cone–rod dystrophies, whereas the M-cone driven ERG responses were even phase advanced. Moreover, the complex origin of the standard 30-Hz flicker ERG and its dependency on S_m and the phase difference between the L- and M-cone driven ERGs implies that the reduction of S_m in the patient population is not a trivial finding despite reduced photopic standard ERG responses. Separation of cone type specific pathways is required to show that both the L- and M-cone driven ERG sensitivity (A_L, A_M) and the global L-/M-cone driven ERG sensitivity (S_m) are reduced in cone and cone–rod dystrophies.

The implicit time of the standard single-flash photopic ERG and the standard 30-Hz flicker ERG is often abnormal in cone and cone–rod dystrophies. In agreement with these observations, the majority of our patients exhibited abnormal implicit times. However, patients carrying mutations in *GUCA1A* (Downes et al., 2001) and *peripherin/RDS* (Fishman et al., 1997) can show normal implicit times for the photopic standard ERG responses. Patient #5 with the Gly170Ser mutation in the *peripherin/RDS* gene exhibited relatively normal overall phases of the L- and M-cone driven ERGs resulting in a distinct *additive* interaction between the two (see Fig. 2B). In agreement with these data, the implicit time of the standard 30-Hz flicker ERG was within normal limits (Table 2). However, for the M-cone driven ERG, this patient exhibited a distinctly negative correlation between phase and cone contrast which has not been observed in normal subjects. This negative correlation of ERG phase and the M-cone contrast that we observed in a subset our patients have also been observed in a patient with high myopia (Usui et al., 1998b) and in patients with RP (Scholl & Kremers, 2000) but never in normal subjects (Kremers et al., 1999). Thus, the phase changes of the L- and M-cone driven ERG provide important information about the pathophysiological mechanisms in cone and cone–rod dystrophies that is not readily available in the standard cone driven ERG. The dependency of the ERG phase on cone contrast can provide additional information.

Recently, we found that patients with Stargardt macular dystrophy did not show a decrease in S_m although there was a significant increase in the inter-individual variability (Scholl et al., 2001). Patients with Best macular dystrophy exhibited even an increased S_m (Scholl et al., 2000). Thus, the L-/M-cone driven ERG sensitivity can contribute to the distinction between different retinal and macular dystrophies.

The phase changes of the L- and M-cone driven ERGs can also contribute to the differential diagnosis between different retinal and macular dystrophies. To pursue this issue in more detail, we compared the phase behavior of the L- and M-cone driven ERGs in different patient groups that were previously described. P_M was significantly phase advanced in patients with rod–cone dystrophy (Scholl & Kremers, 2000), Stargardt macular dystrophy (Scholl et al., 2001), and Best macular dystrophy (Scholl et al., 2000). P_L was significantly phase delayed in patients with rod–cone dystrophy and Stargardt macular dystrophy, but normal in patients with Best macular dystrophy. Therefore the phase changes of the L-cone driven ERGs suggest distinct pathomechanisms in cone dystrophy, cone–rod dystrophy and Stargardt macular dystrophy on the one hand and in Best macular dystrophy on the other hand. It is important to point out that in both Stargardt and Best macular dystrophy the abnormal gene product is expressed across the entire retina and that gene mutations in *ABCA4* that are responsible for Stargardt macular dystrophy (Allikmets et al., 1997; Rivera et al., 2000) have also been observed in families manifesting cone–rod dystrophy and/or atypical RP (Cremers et al., 1998; Martinez et al., 1998).

It is known that there is considerable overlap in the standard ERG data of cone dystrophy and the cone–rod dystrophy patients (Simunovic & Moore, 1998). For S_m, patients with cone dystrophy, cone–rod dystrophy and rod–cone dystrophy exhibited similar reductions. However, the phase differences between L- and M-cone driven ERG responses measured in these three patient subgroups differed significantly (Fig. 5). The subgroup of patients exhibiting additive interactions between L- and M-cone driven ERGs (phase differences smaller than 90°) consisted exclusively of patients with cone dystrophy. In contrast, none of the patients with cone–rod dystrophy exhibited additive interactions. But due to the small sample sizes of the subgroups, a distinction between cone–rod dystrophy and RP is not possible on the basis of our data.

In a large psychophysical study, it was found that the majority of patients with cone and cone–rod dystrophies exhibit marked color vision disturbances the magnitude of which is correlated with the loss of visual acuity (Sadowski & Zrenner, 1997). We can confirm this observation: patients with relatively mild visual acuity loss (e.g. patients #7 and #8) had also mild color vision disturbances (see Table 1). But, these two patients did not show any difference in their cone driven ERGs in comparison with the patients with more severe acuity loss and color vision disturbances. The seeming contradiction between the psychophysical tests and the ERG data may be caused by the fact that a large part of the retina is stimulated in the ERG measurements whereas the psychophysical tests mainly involve the macula. Furthermore, the signals leading to an ERG response and to a visual percept tap different postreceptoral mechanisms (Kremers et al., 2000).

In a recent histopathological study on a patient with cone–rod dystrophy, markedly enlarged cone pedicles were found. Double-labeling experiments showed that all cone types (L-/M-cones and S-cones) had abnormal synapses, whereas the adjacent rod spherules had near-normal fine structure (Gregory, Fariss, Possin, Gregory-Evans, & Milam, 1998). These changes can possibly be revealed by electrophysiological tests that depend on the post-receptoral pathways such as the ERG. Possibly, these histopathological cone alterations are linked to the alterations of the L- and M-cone driven ERG responses.

Acknowledgements

We thank S. Kohl and B. Wissinger for providing the genetic data on the *peripherin/RDS* mutation in patient #7; E. Apfelstedt-Sylla, D. Besch, and M. Seeliger for their clinical assistance; K. Vohrer, C. Reichl, and J. Isensee for technical assistance; R. Vonthein for statistical assistance; and E. Zrenner for general support. This work was supported by Deutsche Forschungsgemeinschaft SCHO 734/1-2 to HPNS and fortüne-Grant 707-0-1 (Tübingen, Germany) to HPNS and JK; DFG (German Research Council) SFB 430/C3 and a DFG Heisenberg fellowship to JK (Kr 1317/5-2).

References

Allikmets, R., Singh, N., Sun, H., Shroyer, N. F., Hutchinson, A., Chidambaram, A., Gerrard, B., Baird, L., Stauffer, D., Peiffer, A., Rattner, A., Smallwood, P., Li, Y., Anderson, K. L., Lewis, R. A., Nathans, J., Leppert, M., Dean, M., & Lupski, J. R. (1997). A photoreceptor cell-specific ATP-binding transporter gene (ABCR) is mutated in recessive Stargardt macular dystrophy. *Nature Genetics, 15*, 236–246.

Berson, E. L., Gouras, P., & Gunkel, R. D. (1968). Progressive cone–rod degeneration. *Archives of Ophthalmology, 80*, 68–76.

Birch, D. G., & Fish, G. E. (1987). Rod ERGs in retinitis pigmentosa and cone–rod degeneration. *Investigative Ophthalmology & Visual Science, 28*, 140–150.

Bresnick, G. H., Smith, V. C., & Pokorny, J. (1989). Autosomal dominantly inherited macular cystrophy with preferential short-wavelength cone involvement. *American Journal of Ophthalmology, 108*, 265–276.

Cremers, F. P., van de Pol, D. J., van Driel, M., den Hollander, A. I., van Haren, F. J., Knoers, N. V., Tijmes, N., Bergen, A. A., Rohrschneider, K., Blankenagel, A., Pinckers, A. J., Deutman, A. F., & Hoyng, C. B. (1998). Autosomal recessive retinitis pigmentosa and cone–rod dystrophy caused by splice site mutations in the Stargardt's disease gene ABCR. *Human Molecular Genetics, 7*, 355–362.

Downes, S. M., Holder, G. E., Fitzke, F. W., Payne, A. M., Warren, M. J., Bhattacharya, S. S., & Bird, A. C. (2001). Autosomal dominant cone and cone–rod dystrophy with mutations in the guanylate cyclase activator 1A gene-encoding guanylate cyclase activating protein-1. *Archives of Ophthalmology, 119*, 96–105.

Estévez, O., & Spekreijse, H. (1982). The "silent substitution" method in visual research. *Vision Research, 22*, 681–691.

Fishman, G. A. (1976). Progressive human cone–rod dysfunction (dystrophy). *Transactions American Academy of Ophthalmology and Otolaryngology, 81*, OP716–OP724.

Fishman, G. A., Stone, E. M., Alexander, K. R., Gilbert, L. D., Derlacki, D. J., & Butler, N. S. (1997). Serine-27-phenylalanine mutation within the peripherin/RDS gene in a family with cone dystrophy. *Ophthalmology, 104*, 299–306.

Goodman, G., Ripps, H., & Siegel, I. M. (1963). Cone dysfunction syndromes. *Archives of Ophthalmology, 70*, 214–231.

Gregory, E. K., Fariss, R. N., Possin, D. E., Gregory-Evans, C. Y., & Milam, A. H. (1998). Abnormal cone synapses in human cone–rod dystrophy. *Ophthalmology, 105*, 2306–2312.

Jacobs, G. H., Neitz, J., & Krogh, K. (1996). Electroretinogram flicker photometry and its applications. *Journal of the Optical Society of America A, 13*, 641–648.

Kellner, U., & Foerster, M. H. (1992). Color electroretinography. A method for separation of dysfunctions of cones. *Documenta Ophthalmologica, 80*, 13–23.

Kellner, U., & Foerster, M. H. (1993). Pattern of dysfunction in progressive cone dystrophies—an extended classification. *German Journal of Ophthalmology, 2*, 170–177.

Kellner, U., Sadowski, B., Zrenner, E., & Foerster, M. H. (1995). Selective cone dystrophy with protan genotype. *Investigative Ophthalmology & Visual Science, 36*, 2381–2387.

Kohl, S., Giddings, I., Besch, D., Apfelstedt, S. E., Zrenner, E., & Wissinger, B. (1998). The role of the peripherin/RDS gene in retinal dystrophies. *Acta Anatomica Basel, 162*, 75–84.

Kremers, J., & Scholl, H. P. N. (2001). Rod-/L-cone and rod-/M-cone interactions in electroretinograms at different temporal frequencies. *Visual Neuroscience, 18*, 339–351.

Kremers, J., Scholl, H. P. N., Knau, H., Berendschot, T. T. J. M., Usui, T., & Sharpe, L. T. (2000). L- and M-cone ratios in human trichromats assessed by psychophysics electroretinography and retinal densitometry. *Journal of the Optical Society of America A, 17*, 517–526.

Kremers, J., Stepien, M. W., Scholl, H. P. N., & Saito, C. A. (2003). Cone selective adaptation influences L- and M-cone driven signals in electroretinography and psychophysics. *Journal of Vision, 3*, 146–160.

Kremers, J., Usui, T., Scholl, H. P. N., & Sharpe, L. T. (1999). Cone signal contributions to electroretinograms in dichromats and trichromats. *Investigative Ophthalmology & Visual Science, 40*, 920–930.

Krill, A. E. (1977). *Hereditary retinal and choroidal diseases*. Hagerstown, Maryland: Harper & Row Publishers Inc.

Krill, A. E., Deutman, A. F., & Fishman, M. (1973). The cone degenerations. *Documenta Ophthalmologica, 35*, 1–80.

Lanthony, P., & Dubois, P. A. (1973). Le Farnsworth 15 désaturé. *Bulletin de la Societe Ophthalmologe de France, 73*, 861–866.

Marmor, M. F., & Zrenner, E. (1998). Standard for clinical electroretinography (1999 update). International Society for Clinical Electrophysiology of Vision. *Documenta Ophthalmologica, 97*, 143–156.

Martinez, M. A., Paloma, E., Allikmets, R., Ayuso, C., del Rio, T., Dean, M., Vilageliu, L., Gonzalez, D. R., & Balcells, S. (1998). Retinitis pigmentosa caused by a homozygous mutation in the Stargardt disease gene ABCR. *Nature Genetics, 18*, 11–12.

Neitz, J., & Jacobs, G. H. (1984). Electroretinogram measurements of cone spectral sensitivity in dichromatic monkeys. *Journal of the Optical Society of America A, 1*, 1175–1180.

Nimsgern, C., Krastel, H., Auffarth, G. U., Eggers, I., & Lang, H. (1998). Standardisierte Prüfung des Rot-, Grün- und Blausinns. Vergleich zwischen Farbfleck- und computergestütztem Testverfahren. *Ophthalmologe, 95*, 559–563.

Padmos, P., & van Norren, D. (1971). Cone spectral sensitivity and chromatic adaptation as revealed by human flicker electroretinography. *Vision Research, 11*, 27–42.

Reichel, E., Bruce, A. M., Sandberg, M. A., & Berson, E. L. (1989). An electroretinographic and molecular genetic study of X-linked cone degeneration. *American Journal of Ophthalmology, 108*, 540–547.

Ripps, H., Noble, K. G., Greenstein, V. C., Siegel, I. M., & Carr, R. E. (1987). Progressive cone dystrophy. *Ophthalmology, 94*, 1401–1409.

Rivera, A., White, K., Stohr, H., Steiner, K., Hemmrich, N., Grimm, T., Jurklies, B., Lorenz, B., Scholl, H. P. N., Apfelstedt-Sylla, E., & Weber, B. H. (2000). A comprehensive survey of sequence variation in the *ABCA4* (*ABCR*) gene in Stargardt disease and age-related macular degeneration. *American Journal of Human Genetics, 67*, 800–813.

Sadowski, B., & Zrenner, E. (1997). Cone and rod function in cone degenerations. *Vision Research, 37*, 2303–2314.

Scholl, H. P. N., & Kremers, J. (2000). Large phase differences between L-cone and M-cone driven electroretinograms in retinitis pigmentosa. *Investigative Ophthalmology & Visual Science, 41*, 3225–3233.

Scholl, H. P. N., Kremers, J., Apfelstedt-Sylla, E., & Zrenner, E. (2000). L- and M-cone driven ERGs are differently altered in Best's macular dystrophy. *Vision Research, 40*, 3159–3168.

Scholl, H. P. N., Kremers, J., Vonthein, R., White, K., & Weber, B. H. (2001). L- and M-cone driven electroretinograms in Stargardt's macular dystrophy-Fundus flavimaculatus. *Investigative Ophthalmology & Visual Science, 42*, 1380–1389.

Simunovic, M. P., & Moore, A. T. (1998). The cone dystrophies. *Eye, 12*, 553–565.

Stockman, A., MacLeod, D. I. A., & Johnson, N. E. (1993). Spectral sensitivities of the human cones. *Journal of the Optical Society of America A, 10*, 2491–2521.

Szlyk, J. P., Fishman, G. A., Alexander, K. R., Peachey, N. S., & Derlacki, D. J. (1993). Clinical subtypes of cone–rod dystrophy. *Archives of Ophthalmology, 111*, 781–788.

Usui, T., Kremers, J., Sharpe, L. T., & Zrenner, E. (1998a). Flicker cone electroretinogram in dichromats and trichromats. *Vision Research, 38*, 3391–3396.

Usui, T., Kremers, J., Sharpe, L. T., & Zrenner, E. (1998b). Response phase of the flicker electroretinogram (ERG) is influenced by cone excitation strength. *Vision Research, 38*, 3247–3251.

van Norren, D., & Padmos, P. (1973). Human and macaque blue cones studied with electroretinograpy. *Vision Research, 13*, 1241–1254.

van Schooneveld, M. J., Went, L. N., & Oosterhuis, J. A. (1991). Dominant cone dystrophy starting with blue cone involvement. *British Journal of Ophthalmology, 75*, 332–336.

Weleber, R. G., Carr, R. E., Murphey, W. H., Sheffield, V. C., & Stone, E. M. (1993). Phenotypic variation including retinitis pigmentosa, pattern dystrophy, and fundus flavimaculatus in a single family with a deletion of codon 153 or 154 of the peripherin/RDS gene. *Archives of Ophthalmology, 111*, 1531–1542.

Williams, D. R., & Roorda, A. (1999). The trichromatic cone mosaic in the human eye. In K. R. Gegenfurtner, & L. T. Sharpe (Eds.), *Color vision: From genes to perception* (pp. 113–122). Cambridge: Cambridge University Press.

Wu, S., Burns, S. A., & Elsner, A. E. (1995). Effects of flicker adaptation and temporal gain control on the flicker ERG. *Vision Research, 35*, 2943–2953.

Yagasaki, K., & Jacobson, S. G. (1989). Cone–rod dystrophy. Phenotypic diversity by retinal function testing. *Archives of Ophthalmology, 107*, 701–708.